Structural and electrical characterization of intrinsic n-type In₂O₃ nanowires

Gunho Jo, Woong-Ki Hong, Jongsun Maeng, Tae-Wook Kim, Gunuk Wang, Ahnsook Yoon,
Soon-Shin Kwon, Sunghoon Song, Takhee Lee *

Department of Materials Science and Engineering, Gwangju Institute of Science and Technology, Gwangju 500-712, Republic of Korea

Abstract

We synthesized high-quality single-crystalline indium oxide nanowires using gold catalytic vapor–liquid–solid growth and characterized their electrical properties with field effect transistor structures. The grown indium oxide nanowires are non-stoichiometric with In:O composition ratio of 1:1.24 due to oxygen vacancies from X-ray photoelectron spectroscopic study. These oxygen vacancies act as donors in indium oxide nanowires. The field effect transistors based on these nanowires exhibited good transistor characteristics with well-defined linear and saturation regions with on/off ratios as high as 3×10^4 at drain bias 0.1 V, electron carrier density of 3.7×10^{17} cm^{-3} and an electron mobility of 85 cm²/V s.
© 2007 Elsevier B.V. All rights reserved.

Keywords: Indium oxide; Nanowire; Field effect transistor; Nanoelectronics

1. Introduction

One-dimensional nanostructures such as nanowires and nanotubes have recently attracted much attention as versatile building blocks for electronics, photonics, nanolasers, light-emitting diodes and solar cells due to their distinctive properties and potential applications. Various semiconducting nanowires of the single element, or III–V and IV compounds including Ge, ZnO, Si, GaN, GaAs, CdO, and In₂O₃ have been successfully synthesized using chemical vapor deposition (CVD) [1,2], pulsed-laser deposition [3], electrochemical deposition [4] or laser ablation [5]. Of these, In₂O₃ nanowires as a wide-bandgap semiconductor (a direct bandgap of 3.55–3.75 eV and an indirect energy gap of 2.62 eV) have been extensively studied for advanced applications in electronic, optoelectronic, photo-detectors, memory devices, and high sensitivity sensors [6–8]. It is therefore important to be able to synthesize high-quality In₂O₃ nanowires, preferentially in the single-crystalline form, for electronic properties studies and potential applications.

In recent years, synthetic doping control of In₂O₃ nanowires [9] and their properties such as electronic transport characteristics [10], biosensing [8], and photoluminescence were investigated [11]. We synthesized In₂O₃ nanowires using the carbothermal reduction method. This leads to non-stoichiometric composition in the nanowire due to oxygen vacancies created during the growth, studied by X-ray photoelectron spectroscopy (XPS). We also fabricated the In₂O₃ nanowire field effect transistors (FETs) and subsequently characterized their electronic transport properties. The In₂O₃ nanowires with oxygen deficiency showed the n-type behavior from gate-dependent transistor characteristics with good transistor performances of on/off ratio and mobility.

2. Experiment

The In₂O₃ nanowires used in this study were made by carbothermal reduction followed by the catalyst-mediated heteroepitaxial growth technique [12]. First, a mixture of In₂O₃ powder (99.995%) and graphite powder (99%) in a 4:1 weight ratio was placed into a quartz boat inside a tube reactor. Then, In₂O₃ nanowires were grown on a Si/SiO₂ substrate covered with 2 nm gold film as a catalyst for nanowire synthesis. During the nanowire growth, the temperature was set at 900–1000 °C, while Ar mixed with 5% O₂ was flowing at a rate of 50–100 sccm for ~35 min. After cooling, the structural properties of the nanowires were characterized using scanning electron microscopy (SEM), transmission electron microscopy

* Corresponding author. Tel.: +82 62 970 2314; fax: +82 62 970 2304.
E-mail address: tlee@gist.ac.kr (T. Lee).

(TEM), electron diffraction, X-ray diffraction (XRD), and X-ray photoelectron spectroscopy.

To fabricate In_2O_3 nanowire FET devices, the as-grown nanowires were sonicated in isopropyl alcohol solution for 2–3 min, and then the suspension was dropped onto a highly doped p-type silicon substrate with a 100 nm thick thermally grown oxide. This highly doped silicon substrate can serve as a back gate electrode to modulate the carrier density in the nanowire. Source and drain electrodes with spacing of 2–3 μm were defined by photolithography, followed by electron beam evaporation of Ti/Au (30/50 nm). After lift-off, the device was carefully cleaned and electrical transport measurements were made at room temperature with semiconductor parameter analyzer (HP-4155C).

3. Results and discussion

Fig. 1(a) shows a typical field-emission scanning electron microscopy (FESEM) image of In_2O_3 nanowires grown on the Si/SiO$_2$ substrate with Au nanoclusters. These nanowires have diameters in the range of 10–100 nm and lengths extending to 5 μm or more from TEM and SEM analysis. The crystal structures of these nanowires were examined using XRD. There are three major diffraction peaks, as shown in Fig. 1(b). They can be indexed as (2 2 2), (4 0 0), and (4 4 0) crystal planes of a cubic structure with a lattice constant of a = 1.0 nm (from JCPDS Card No. 44-1087). The structural analysis of the In_2O_3 nanowires was characterized using TEM and electron diffraction patterns (Fig. 1(c), inset). Fig. 1(c) shows a typical TEM image of a single 30 nm diameter nanowire with an Au catalyst. High-resolution

TEM (HR-TEM) image of Fig. 1(d) shows that this nanowire is single-crystalline with an interplanar spacing of 0.5 nm in the [1 0 0] direction.

In addition to the structural information, XPS measurements were carried out in order to investigate the composition of indium oxide nanowires. The XPS spectra shown in Fig. 2(a) depict the full range scanned from 0 to 1200 eV. Peaks such as C, O1s, Si, In3p, In3d, In4s, In4p, and In4d were detected. The zoomed-in XPS spectra for the O1s signals in Fig. 2(b) indicate that the binding energy is 530.3 eV, which is consistent with that of O1s in In_2O_3 and 532.3 eV, indicates that Si bonding with O in Si/SiO$_2$ substrate. And, Fig. 2(c) shows the peaks of 452.3 eV for In3d$_{3/2}$ and 444.8 eV for In3d$_{5/2}$, respectively. The In:O composition ratio in indium oxide nanowires was found as 1:1.24, based on the quantitative analysis from the XPS spectra, suggesting that the nanowires are non-stoichiometric. The most probable explanation of this non-stoichiometric composition is the formation of the oxygen vacancies during the growth of nanowires. The indium oxides close to stoichiometric In_2O_3 have a low free carrier concentration and high resistivity ($\sim 10^8$ Ω cm), which is more like insulator [13]. However, non-stoichiometirc indium oxide nanowires have high free carrier concentration, thus more conducting, which is due to oxygen deficiency. In other words, there are oxygen vacancies in the non-stoichiometirc indium oxide of structure like In_2O_{3-x}, where x is the deviation from stoichiometry. The electrical conductivity of non-stoichiometirc indium oxide nanowires arises from oxygen vacancies which act as donors of electrons to the conduction band [8,13–15].

In order to investigate the electrical properties of these non-stoichiometirc indium oxide nanowires, we fabricated
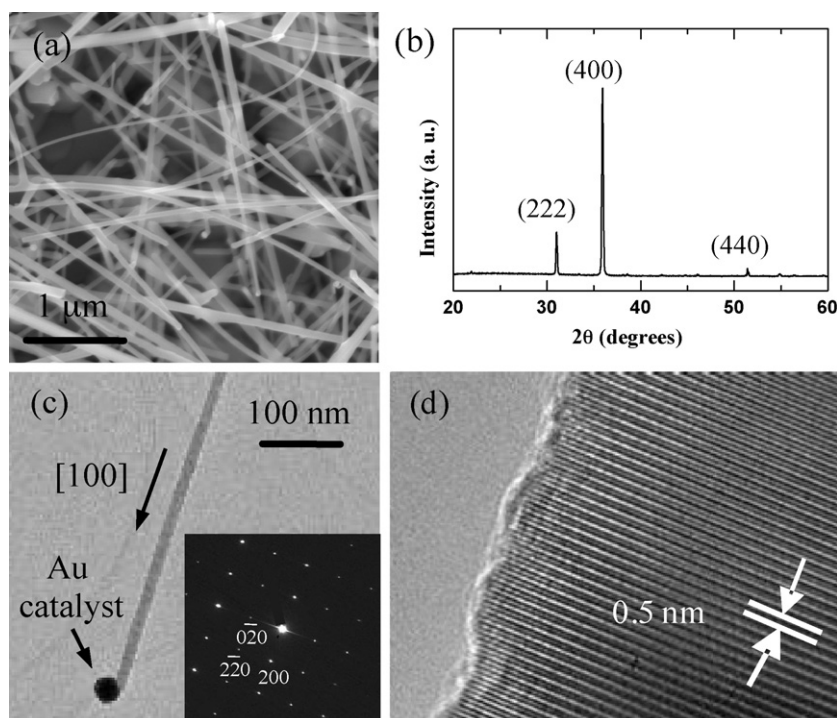
Fig. 1. (a) FESEM image of In_2O_3 nanowires grown from Au nanoclusters on SiO$_2$/Si substrate. (b) XRD pattern of In_2O_3 nanowires. (c) TEM image of an individual In_2O_3 nanowire showing its [1 0 0] growth direction with an Au catalyst. Inset is the electron diffraction pattern recorded along the $\langle 0\,0\,1 \rangle$ zone axis. (d) HRTEM image of the In_2O_3 nanowire with the lattice spacing of 0.5 nm.
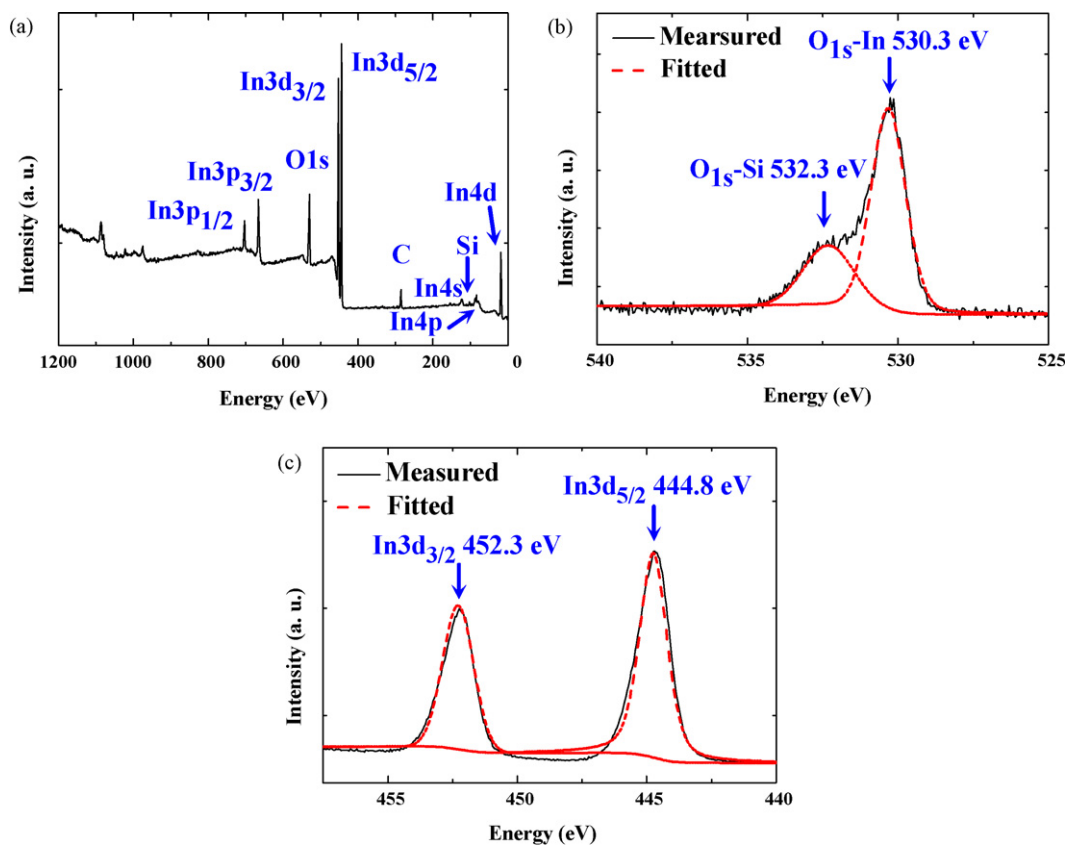
Fig. 2. (a) XPS spectra of the In_2O_3 nanowires. XPS spectra in zoomed-in selected regions for oxygen signals (b) and for indium signals (c).

the nanowires into FET device structures. The schematic structure of the nanowire FET is illustrated in Fig. 3(a). Fig. 3(b) shows a series of optical and FESEM images of the In_2O_3 nanowire FET devices. From left to right images, we show zoomed-in pictures of an In_2O_3 nanowire FET with the channel length around 3 μm between sources and drain electrode.

Fig. 4(a) shows source-drain current versus voltage ($I_{DS}-V_{DS}$) characteristics obtained from a single In_2O_3 nanowire

FET at different gate voltages (V_G) from −1.5 to 2.5 V with 0.5 V step. For $V_G \geq -1.0$ V, I_{DS} increases almost linearly up to the saturation region. The linear relationship of $I_{DS}-V_{DS}$ at low bias indicates good ohmic contact to the nanowire with low contact resistance. The gate-dependence of the $I_{DS}-V_{DS}$ curves (Fig. 4(b)) also showed that In_2O_3 nanowire FETs are n-type, that is, the conductance of the nanowire increase (decrease) with increasingly positive (negative) gate voltages. As explained previously, we can attribute the n-type behavior of undoped In_2O_3
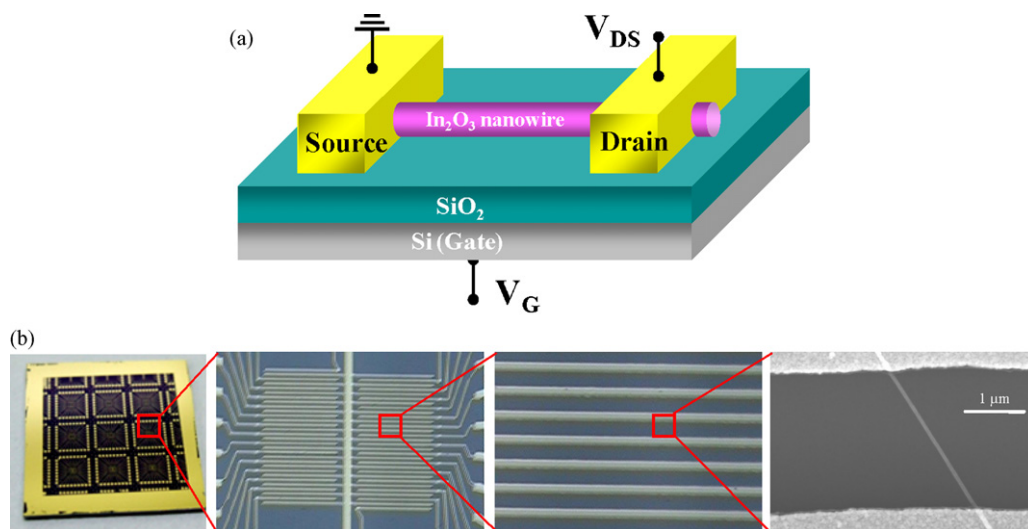
Fig. 3. (a) The schematic diagram of the In_2O_3 nanowire FET device; (b) optical and SEM images for fabricated In_2O_3 nanowire FET devices.
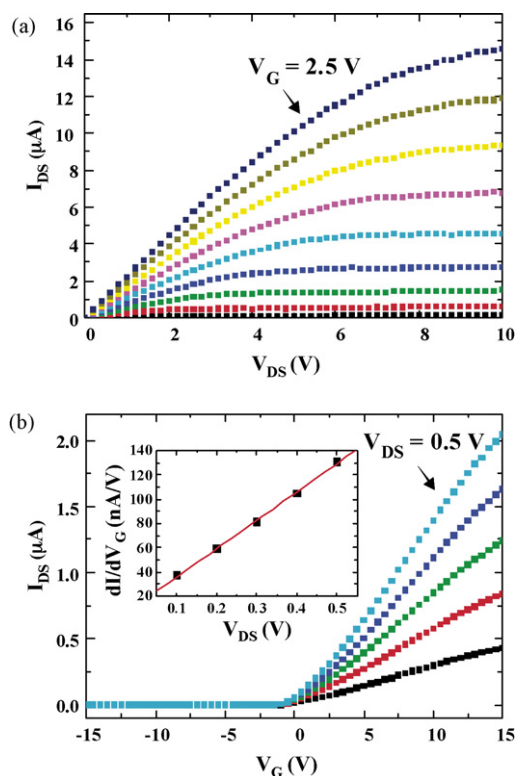
Fig. 4. (a) I_{DS}–V_{DS} data for V_G from −1.5 to 2.5 V with 0.5 V step, acquired from a 30 nm diameter In_2O_3 nanowire FET. (b) I_{DS}–V_G data for V_{DS} from 0.1 to 0.5 V with 0.1 V step. (Inset) Transconductance dI_{DS}/dV_G vs. V_{DS}.

nanowires to the oxygen deficiency, from XPS characterization (Fig. 2).

We investigated the transfer characteristics of the In_2O_3 nanowire FETs by measuring the source-drain current versus gate voltage (I_{DS}–V_G) curves, as shown in Fig. 4(b). The on-to-off current ratio I_{ON}/I_{OFF} was found as 3×10^4 (at $V_{DS} = 0.1$ V) to 5.6×10^5 (at $V_{DS} = 0.5$ V) from this plot. These values show better performance than previously reported In_2O_3 nanowire FETs [7,10]. The carrier concentration can be estimated from the total charge, $Q_{tot} = CV_T$ in the nanowire, where C is the nanowire capacitance and V_T is the threshold voltage (−0.5 V). The approximate nanowire capacitance C is $2\pi\varepsilon\varepsilon_0 L/\ln(2h/r)$, where ε is dielectric constant of SiO_2 (3.9), h is the thickness of the SiO_2 layer (100 nm), L is the length (3 μm), and r is radius of In_2O_3 nanowire (15 nm). Then, the electron carrier density, $n_e = Q_{tot}/(e\pi r^2 L)$, was found as 3.7×10^{17} cm^{-3} for this nanowire FET device. The mobility of the carriers was also estimated from transconductance, $dI/dV_G = \mu(C/L^2)V_{DS}$, where μ is the carrier mobility [16] and found to be 85 cm^2/V s from dI/dV_G

versus V_{DS} curve (Fig. 4(b), inset). This mobility is comparable to the reported values for P-doped Si nanowires [17].

4. Conclusion

We have synthesized single-crystalline indium oxide nanowires using the carbothermal reduction method. These nanowires are non-stoichiometric with In:O composition ratio of 1:1.24, studied from XPS characterization. We have shown that the grown non-stoichiometric In_2O_3 nanowires are n-type behavior due to oxygen vacancies which act as donors of electrons to the conduction band. These indium oxide nanowire transistors have exhibited good transistor characteristics with well-defined saturation regions and high on-off current ratio and mobility.

Acknowledgements

References

[1] M.H. Huang, S. Mao, H. Feick, H. Yan, Y. Wu, H. Kind, E. Weber, R. Russo, P. Yang, Science 292 (2001) 1897.
[2] J. Xiang, W. Lu, Y. Hu, Y. Wu, H. Yan, C.M. Lieber, Nature 441 (2006) 489–493.
[3] O. Hayden, A.B. Greytak, D.C. Bell, Adv. Mater. 17 (2005) 701.
[4] M. Law, L.E. Greene, J.C. Johnson, R. Saykally, P. Yang, Nat. Mater. 4 (2005) 455.
[5] C. Li, D. Zhang, S. Han, X. Liu, T. Tang, C. Zhou, Adv. Mater. 15 (2003) 143.
[6] C. Li, M. Curreli, H. Lin, B. Lei, F.N. Ishikawa, R. Datar, R.J. Cote, M.E. Thompson, C. Zhou, J. Am. Chem. Soc. 127 (2005) 12484.
[7] P. Nguyen, Hou T. Ng, T. Yamada, M.K. Smith, J. Li, J. Han, M. Meyyappan, Nano Lett. 4 (2004) 651.
[8] C. Li, W. Fan, D.A. Straus, B. Lei, S. Asano, D. Zhang, J. Han, M. Meyyappan, C. Zhou, J. Am. Chem. Soc. 126 (2004) 7750.
[9] B. Lei, C. Li, D. Zhang, T. Tang, C. Zhou, Appl. Phys. A 79 (2004) 439.
[10] D. Zhang, C. Li, S. Han, X. Liu, T. Tang, W. Jin, C. Zhou, Appl. Phys. Lett. 82 (2003) 112.
[11] C.L. Hsin, J.H. He, L.J. Chen, Appl. Phys. Lett. 88 (2006) 063.
[12] J.Y. Lao, J.Y. Huang, D.Z. Wang, Z.F. Ren, Adv. Mater. 16 (2004) 1.
[13] B. Mohagheghi, B. Mohagheghi, M.S. Saremi, Semicond. Sci. Technol. 18 (2003) 97.
[14] T. Skála, K. Veltruská, M. Moroseac, I. Matolínová, G. Korotchenkov, V. Matolín, Appl. Surf. Sci. 205 (2002) 196.
[15] S.B. Zhang, S.-H. Wei, Alex Zunger, Phys. Rev. B 63 (2001) 075205.
[16] Y. Huang, X. Duan, Y. Cui, C.M. Lieber, Nano Lett. 2 (2002) 101.
[17] G. Zheng, W. Lu, S. Jin, C.M. Lieber, Adv. Mater. 16 (2004) 21.